Journal of Alloys and Compounds 506 (2010) 400–406

Contents lists available at ScienceDirect

Journal of Alloys and Compounds

journal homepage: www.elsevier.com/locate/jallcom

Development of cobalt ferrite powder preparation employing the sol–gel technique and its structural characterization

M. Sajjia [a,*], M. Oubaha [b], T. Prescott [a], A.G. Olabi [a]

[a] School of Mechanical and Manufacturing Engineering, Dublin City University, Glasnevin, Dublin 9, Ireland
[b] Optical Sensor Laboratory, National Centre for Sensor Research, Dublin City University, Glasnevin, Dublin 9, Ireland

ARTICLE INFO

Article history:
Received 24 March 2010
Received in revised form 30 June 2010
Accepted 6 July 2010
Available online 17 July 2010

Keywords:
Sol–gel
Cobalt ferrite nanoparticles
Spinel structure
Crosslinker
Chelating agent

ABSTRACT

This work focuses on the development of a method to make cobalt ferrite powder using the sol–gel process. A particular emphasis is devoted to the understanding of the role of the chemical parameters involved in the sol–gel technique, and of the heat treatment on the structures and morphologies of the materials obtained. Several samples of cobalt ferrite powder were obtained by varying the initial parameters of the process in addition to the heat treatment temperature. X-ray diffraction and scanning electron microscopy were used to identify the structure and morphology of samples demonstrating the influence of the initial parameters. DTA/TGA was carried out on two standard samples to identify important reaction temperatures during the heat treatment. The average size of the nano crystallites was estimated for a sample by the full width at half maximum (FWHM) of the strongest X-ray diffraction (XRD) peak. It has been found that the chelating agent and the crosslinker have a critical influence on the resultant structure, the particle size and the particle size distribution.

1. Introduction

Cobalt ferrite nanoparticles have recently become the subject of research interest from the point of view of the synthesis, the structure, the magnetic characterization, and the application [1–4]. In particular, interest in cobalt ferrite powder as a ferrimagnetic material has arisen due to its unique properties e.g. very high resistivity, a positive anisotropy constant, and a high magnetostriction [5,6] which is defined as the change in the shape under the effect of magnetic field [7–9]. These properties could make cobalt ferrite a potential candidate for many applications e.g. high frequency magnets, information storage systems, magnetic bulk cores, microwave absorbers [10] and biomedical applications, such as magnetic hyperthermia, drug delivery, magnetic resonance imaging, and biosensors [11,12]. However, the magnetic properties of cobalt ferrite particles have been found to be crucially dependent on the size, shape and purity of these particles, which in turn are dependent on the initial parameters adopted in the process of producing these particles which can change the subsequent microstructure of the material. Baldi et al. [13] concluded that cobalt ferrite nanoparticles synthesized using the polyol method offer the possibility to optimize the heat release capability of magnetic fluid hyperthermia (MFH) mediators at a given frequency over a wide range, just by finely tuning the average particle size. Methods for making cobalt ferrite nanoparticles are very diverse including the polymeric precursor method [14], wet chemical routes [15], microemulsions [16], and chemical co-precipitation techniques [17,18]. Nanoparticles prepared by these processes have different saturation magnetization and coercivity values depending on the particle size distribution. Generally, the size of these nanoparticles was found to be dependent on the heat treatment temperature.

The sol–gel process is one of solution-phase chemical methods which can provide the means of producing high purity, crystalline nanoscale materials of a particular size. The sol–gel technique is probably the most effective method for the synthesis of homogeneous nano-sized particles. This process offers the possibility of a generalized approach to the production of both single and complex oxide nanoparticles [19,20]. It was used in preparing composite materials containing highly dispersed magnetic cobalt ferrite nanoparticles as core particles in a silica matrix [21,22]. Silva et al. [23] had already found that the size of cobalt ferrite particles formed in the silica matrix increases with an increase in the heat treatment temperature, leading to an increase in the saturation magnetization and coercivity.

The sol–gel process is a liquid phase synthesis involving hydrolysis and condensation reactions of metal precursors, such as salts or alkoxides, leading to the formation of three-dimensional inorganic networks [24]. The hydrolysis allows the formation of hydroxyl groups (M–OH) that subsequently condense into strong and rigid metal–oxo–metal bridges (M–O–M), and the second of the reactions is generally irreversible.

* Corresponding author. Tel.: +353 17007563; fax: +353 17005345.
E-mail address: sajjiam2@mail.dcu.ie (M. Sajjia).

0925-8388/$ – see front matter © 2010 Elsevier B.V. All rights reserved.
doi:10.1016/j.jallcom.2010.07.015

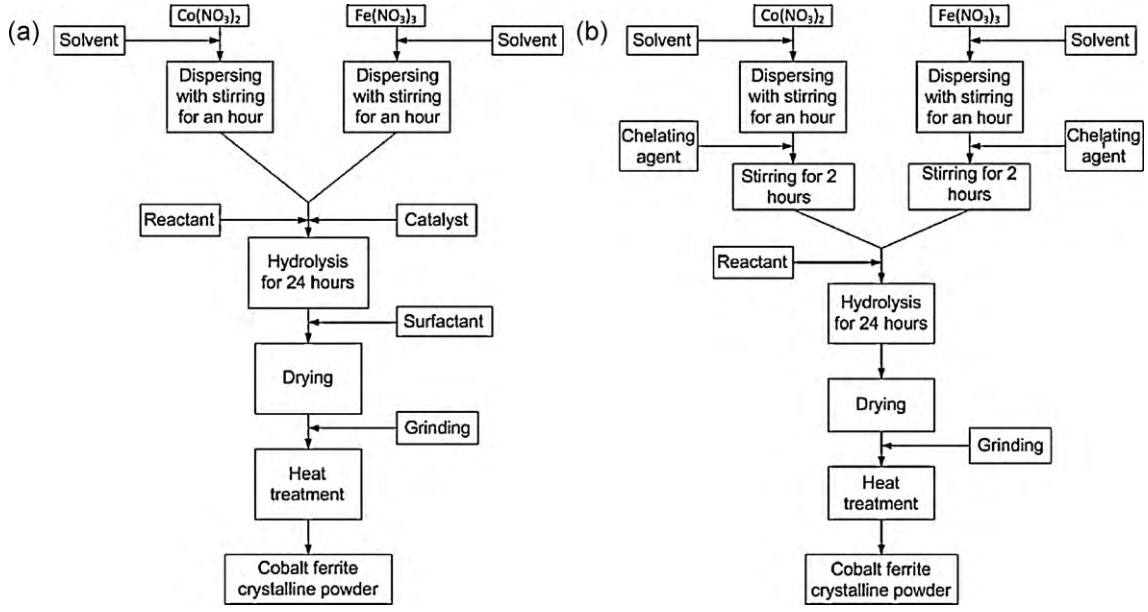

Fig. 1. Materials preparation.

To our knowledge, none has focused on a fundamental understanding of the influence of the various chemical parameters on the final structure and morphology of the materials obtained. Therefore, the aim of this paper is to address this gap in understanding by concentrating in particular on the effect of the nature of the hydrolysis and also on the effect of both the chelating agent and the crosslinker. Conclusions regarding the influence of the composition of the starting solution and subsequent heat treatment were drawn with reference to macroscopic observation of the materials and in conjunction with their XRD patterns.

2. Experimental

2.1. Material development

The sol–gel synthesis was based on the formation of a stable and homogenous sol obtained from a mixture of Cobalt (II) nitrate hexahydrate, ($Co(NO_3)_2 \cdot 6H_2O$, ≥99%, Fluka) and Iron (III) nitrate nonahydrate, ($Fe(NO_3)_3 \cdot 9H_2O$, ≥98%, Sigma–Aldrich). The precursors were used as received without any further refinement. 0.1 M Sodium hydroxide solution and de-ionized water were used as a catalyst and a reactant respectively. Di (ethylene glycol) diacrylate (DEGDA, Sigma–Aldrich) and citric acid (CA, Sigma–Aldrich) were employed as the crosslinker and the chelating agent respectively. The role of the crosslinker was to bring closer together the different inorganic particles and to improve the homogeneity of the solution. The chelating agent on the other hand reacts with both precursors by blocking their reactive functions achieving a remarkably homogeneous mixture.

The investigation of the effect of the crosslinker and the chelating agent was carried out to provide a good understanding about their influence on the structure and morphology. In all studies, the molar ratio $Co(NO_3)_2 \cdot 6H_2O$:$Fe(NO_3)_3 \cdot 9H_2O$ was kept constant at 1:2 and the hydrolysis was brought to 100% completion.

Two main procedures as shown in Fig. 1(a) and (b) were employed in this study. In the first procedure, Fig. 1(a), after the $Co(NO_3)_2$ and $Fe(NO_3)_3$ had been separately dispersed in a solvent and stirred for an hour both solutions were mixed together at that stage followed by the addition of the reactant and the catalyst. The mixture was then left stirring for 24 h. Later when appropriate, the crosslinker was added. And then the sol was stirred for further 15 h. In the second procedure, Fig. 1(b), after the $Co(NO_3)_2$ and $Fe(NO_3)_3$ had been separately dispersed in a solvent and stirred using magnetic stirrers for an hour the chelating agent was added and the two mixtures were stirred for 2 more hours. Both solutions were then mixed together and stirring was continued for 24 more hours. Stirring allowed the hydrolysis and condensation reactions to take place. All sols obtained by these procedures were stable and homogeneous showing the success of the sol–gel synthesis. The sols were then dried at 100 °C for 12 h under ambient atmosphere, and annealed in a Horizontal Tube furnace (Carbolite Ltd., Sheffield, UK) between 600 °C and 1000 °C. Details of all the samples are listed in Table 1 with related synthesis parameters and conditions.

Samples (1–9) were prepared employing the first procedure (a) and samples (10–14) were prepared employing the second procedure (b). 0.1 M Nitric Acid solution was used as a catalyst for samples 3 and 4 to investigate any possible different effect when changing the catalyst from basic to acidic.

2.2. Characterization

The structural characterization of all samples was carried out by (D8 ADVANCE-BRUKER) X-ray diffraction (XRD) using Cu Kα radiation. The machine is connected

Table 1
Samples with their initial parameters and conditions.

Sample	Solvent	Molar ratio (%)			Heat treatment temperature in °C (for 10 h)
		Crosslinker/metal ions	Reactant/metal ions	Chelating agent/metal ions	
1	2-Propanol	–	100	–	600
2	2-Propanol	50	100	–	600
3	De-ionized water	–	–	–	600
4	De-ionized water	50	–	–	600
5	De-ionized water	–	–	–	600
6	De-ionized water	50	–	–	600
7	2-Propanol	300	100	–	600
8	2-Propanol	300	100	–	800
9	2-Propanol	300	100	–	1000
10	2-Propanol	–	100	100	600
11	2-Propanol	–	100	100	600
12	De-ionized water	–	–	100	600
13	De-ionized water	–	–	100	1000
14	De-ionized water	–	–	200	600

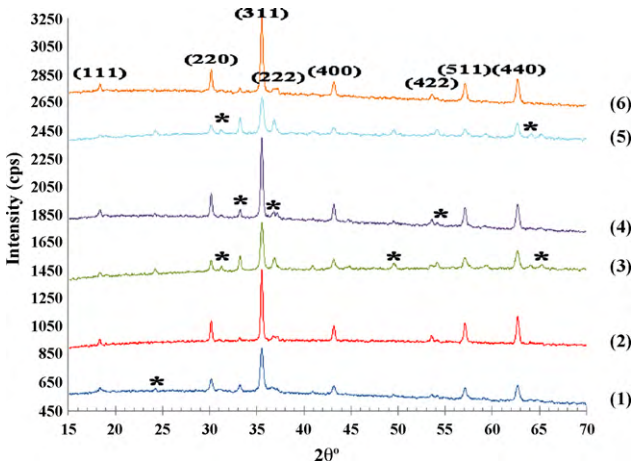

Fig. 2. XRD patterns of samples (1–6).

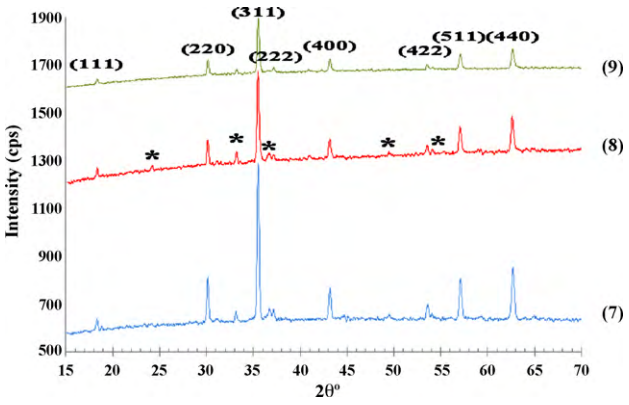

Fig. 3. XRD patterns of samples (7–9).

to a computer with a package of associated softwares called (DIFFRAC PLUS Evaluation). One of those softwares called (EVA), which has database of all materials' XRD patterns of the periodic table and their possible alloys, was used to determine the identity and to provide an indication of the concentration of each phase in the samples by comparing the obtained XRD patterns with the pure cobalt ferrite XRD pattern from the database then calculations of differences considering other possible XRD patterns give the quality and the quantity of present phases. Differential thermal analysis (DTA) and thermo-gravimetric analysis (TGA) were carried out in air to estimate the temperatures at which the decomposition and oxidation of the crosslinker and the chelating agent take place. The morphology of the materials (homogeneity and particle size) was observed by a scanning electron microscope (SEM) and a field emission-scanning electron microscope (FE-SEM).

3. Results

3.1. XRD patterns

According to the literature [17,25], the cobalt ferrite pattern exhibits eight peaks located between $2\theta^\circ = 15$ and $2\theta^\circ = 70$ as follows: 18.289, 30.085, 35.438, 37.057, 43.059, 53.446, 56.975, 62.587. The respective intensities of these peaks presented with respect to the most intense peak located at $2\theta^\circ = 35.438$ are as follows: 10%, 30%, 100%, 8%, 20%, 10%, 30%, 40%, where the related Miller indices are: (1 1 1), (2 2 0), (3 1 1), (2 2 2), (4 0 0), (4 2 2), (5 1 1), (4 4 0) respectively.

The XRD patterns of samples 1–6, as shown in Fig. 2, show all peaks related to the $CoFe_2O_4$ phase proving the attainment of cobalt ferrite structure. However, additional peaks were observed in these XRD patterns demonstrating the presence of other phases beside the cobalt ferrite structure, which have been attributed to the following impurities, hematite (Fe_2O_3), iron oxide (Fe_3O_4) in addition to cobalt oxides (Co_3O_4) and (CoO) with (JCPDS-ICDD) file numbers of (89-2810), (26-1136), (42-1467) and (71-1178) respectively as investigated using (EVA) software. In other words, there is no doubt cobalt ferrite structure is attained as XRD patterns show. Furthermore, the formation of iron oxides on one side means the formation of cobalt oxides on the other side which kept the stoichiometry unaltered. Moreover, if for instance iron oxide formed and cobalt oxide did not form, that would have meant the change in the initial stoichiometry. The presence of oxides indicates that the reaction between the constituents was incomplete. The results vary; however samples 2, 4, and 6, which were made with the crosslinker, contain around 20% less impurity than samples made without the crosslinker.

XRD patterns of samples 7–9, which were prepared with 3 mol crosslinker for 1 mol of mineral ions (Co + Fe), are shown in Fig. 3.

These patterns are (almost) similar to those of samples 2, 4, and 6, indicating the negligible effect of increasing the amount of crosslinker added on the resultant structure. In addition, heat treatment at higher temperatures (800 °C and 1000 °C) for 10 h did not significantly contribute to any reduction in the amount of impurities, which seems to be due to an incomplete reaction.

XRD patterns of samples 10–13 prepared using citric acid as a chelating agent with 1:1 (metal ions:citric acid) stoichiometry molar ratios are shown in Fig. 4. A further centrifugation step at 4000 rpm for 20 min was applied to sample 11 in order to remove the supernatant, and to increase the rate of reactions promoting the gelling process in the heavier material at the bottom of the centrifuge tubes.

A quantitative analysis reveals that sample 10 and 12 contain approximately 1% of impurities whereas sample 11 contains over 75% of impurities demonstrating the strong modification of the initial stoichiometry due to centrifugation. On the other hand, sample 13 is composed of 100% pure $CoFe_2O_4$ indicating that the increase in the annealing temperature allowed the disappearance of impurity phases in this particular formulation.

The XRD pattern of sample 14, prepared employing a full chelation to the mineral ions, is shown in Fig. 5. This was to investigate the effect of completely isolating the cations from further reactions during the sol development process. The effect can only be studied by making observations on the powder produced. It is clearly observed that the cobalt ferrite structure was obtained as a single phase, which matches with (JCPDS-ICDD) file number of (22-1086). Heat treatment at 600 °C for 10 h was enough to obtain the pure cobalt ferrite structure for this composition, which leads to the conclusion that the chelating agent had an important effect on reducing the temperature needed during heat treatment to attain the cobalt ferrite structure.

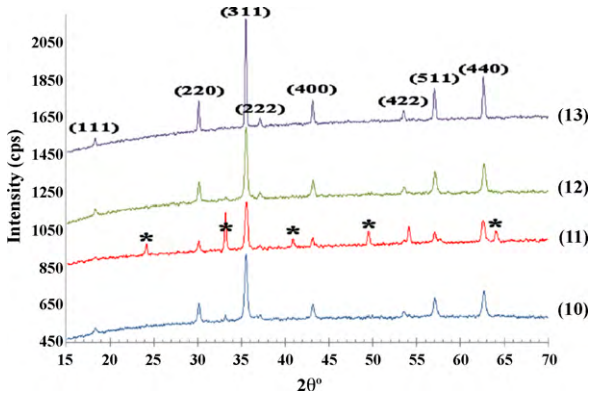

Fig. 4. XRD patterns of samples (10–13).

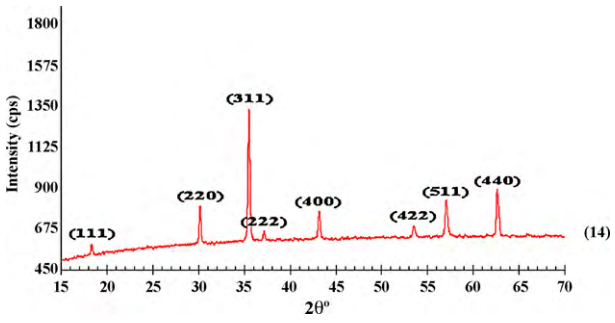

Fig. 5. XRD pattern of sample (14).

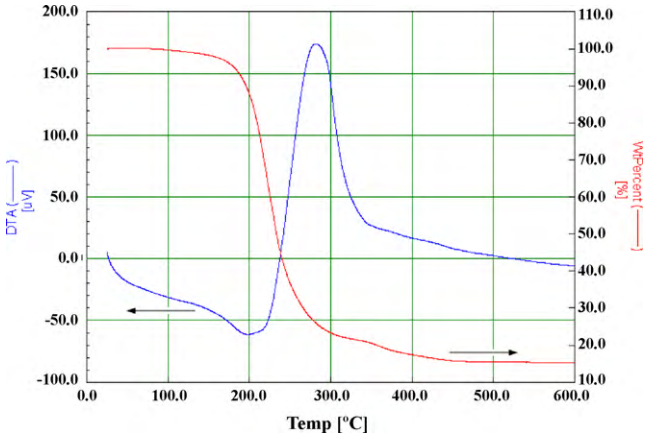

Fig. 6. DTA/TGA curves of sample (9).

3.2. DTA/TGA

DTA/TGA curves of sample 9 are shown in Fig. 6. Over the temperature range 25–600 °C, the DTA curve exhibits only one single exothermic peak at 260 °C which signifies both the decomposition and the oxidation of the crosslinker, or its decomposition products. It is fact that the crosslinker burns when heated releasing carbon dioxide.

DTA/TGA curves of sample 14 are shown in Fig. 7. When heating over 150 °C, citric acid decomposes through the loss of water and carbon dioxide. However, DTA curve exhibits two exothermic peaks, one at 150 °C which refers to the evaporation of the water

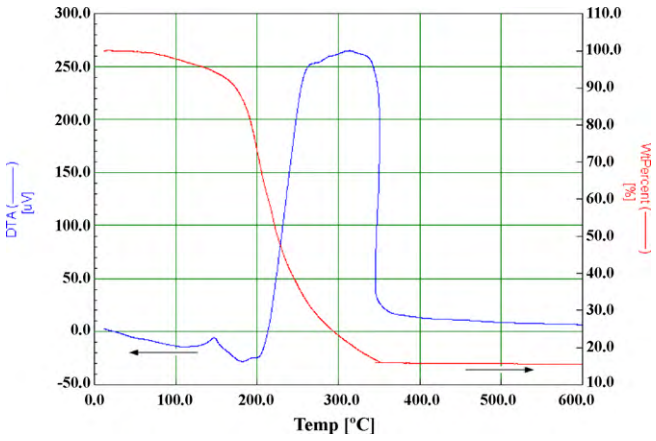

Fig. 7. DTA/TGA curves of sample (14).

compound of citric acid, and the other at 260 °C which refers to the oxidation of carbon content by oxygen in the air and forming carbon dioxide, releasing heat.

3.3. SEM images

SEM images of samples synthesized with (2, 4, 6) and without crosslinker (1, 3, 5) are shown in Fig. 8. Samples prepared with crosslinker exhibit a polydisperse distribution with particle size ranging from 90 nm to 200 nm, while samples synthesized without crosslinker show a monodisperse distribution with particle size around 90 nm; furthermore, some particles were agglomerated and formed large clusters. No difference on both structure and particle size was observed when using different catalyst on relative samples, 3 and 5, 4 and 6 respectively.

SEM images of samples 7–9 are shown in Fig. 9. It indicates that sample 7 has a wider range of particle sizes (50–350 nm). Moreover, particles are larger in size and have a wider size range when the temperature of the heat treatment is increased as shown for samples 8 and 9.

The SEM image of sample 10 is shown in Fig. 10. It shows a nano polydisperse distribution of particles with a range from 80 nm to 200 nm.

An FE-SEM picture of sample 14 is shown in Fig. 11. It indicates the effect of increasing the percentage of CA which results in a wider range of particle sizes (from 20 nm to 250 nm).

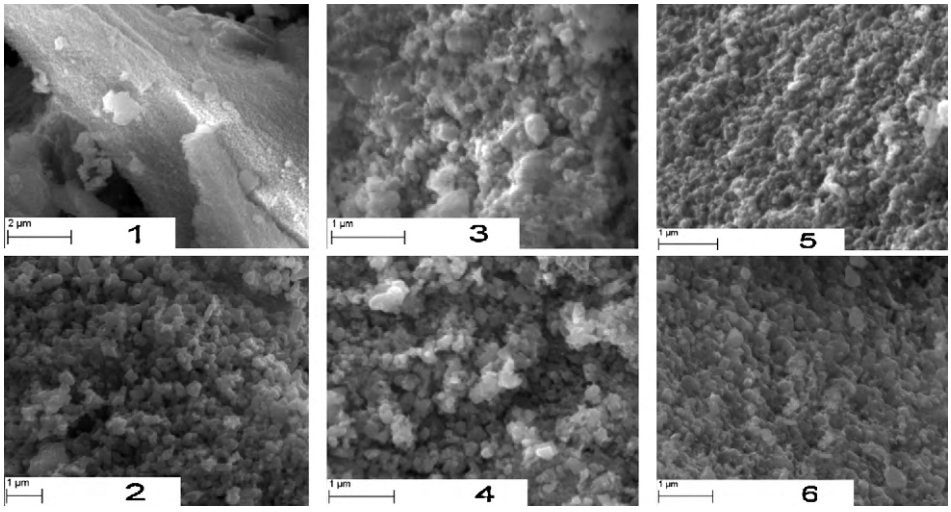

Fig. 8. SEM images of samples (1–6).

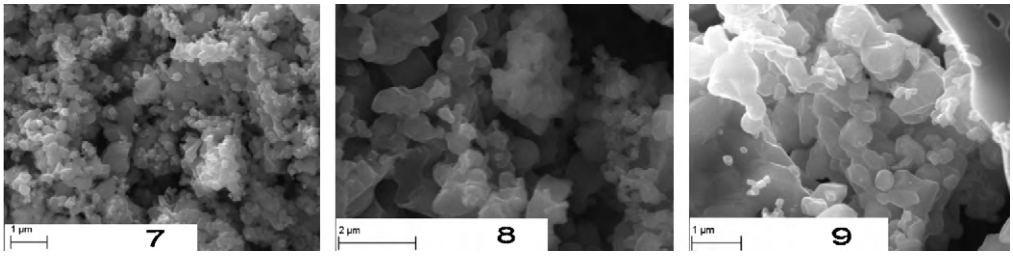

Fig. 9. SEM images of samples (7–9).

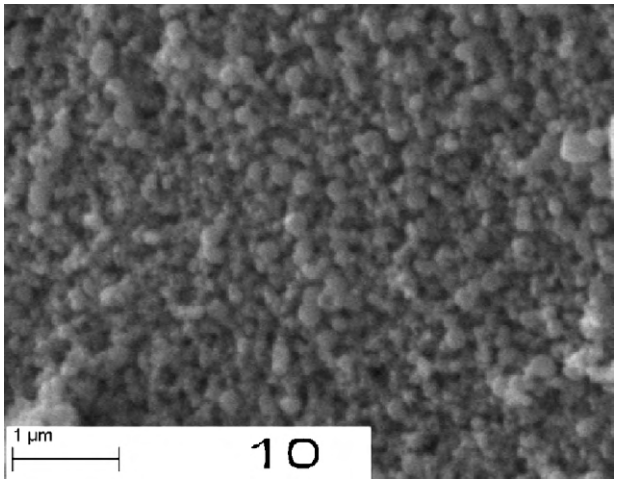

Fig. 10. SEM image of sample (10).

4. Discussion

4.1. Effect of the crosslinker

A comparison of samples prepared with, and without, crosslinker allows two main conclusions to be drawn. Firstly, when employing the same heat treatment conditions, the crosslinker permits the decrease of the impurities by only 20%. Increasing the ratio of the amount of crosslinker with respect to the inorganic part beyond a certain point, to 3:1, did not help in obtaining a purer cobalt ferrite structure.

A calculation using EVA software indicates the presence of 3% of impurities which were identified above as a mixture of other oxides. These results show that along with the formation of cobalt ferrite, the crosslinker also favours the auto-condensation of iron and cobalt colloids to form Fe_2O_3 and CoO. The crosslinker allows different mineral species, firstly to react with the crosslinker, and then subsequently during the heat treatment stage to approach one another and eventually form an oxide bridge, As illustrated in Fig. 12, the cobalt ferrite phase is produced as a result of reaction (b), whereas impurities, that is the other oxides, are a result of reactions (a) and (c). While (b) might be favourable, (a) and (c) can also occur. The impurities probably occur because of the peculiar property of this crosslinker that allows all three different reactions to take place without a sufficiently selective policy, permitting only reaction (b). Therefore, using different ratios of crosslinker resulted in the same final structure.

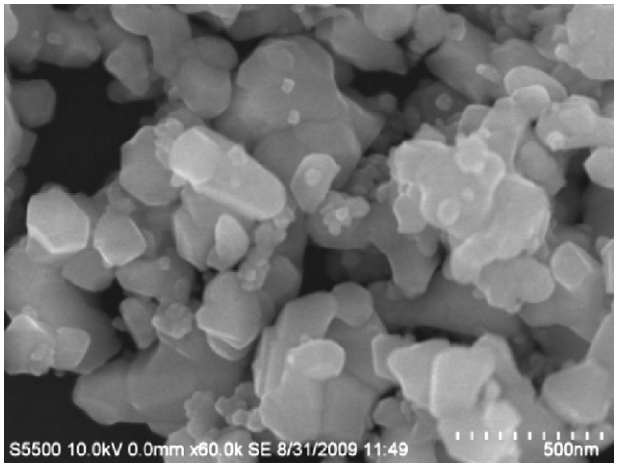

Fig. 11. FE-SEM image of sample (14).

Even when employing heat treatment at higher temperatures (up to 1000 °C), a similar result was obtained. This indicates that the thermal energy was not sufficient to achieve a significant mobility for the cations within the oxides to change positions and so achieve the formation of cobalt ferrite.

Secondly, from a morphological point of view, it is observed that increasing the amount of the crosslinker increases the absolute particle size range from 110 nm to 300 nm when using molar ratios of 50% and 300% with regard to metal ions respectively. In addition, it was found that increasing the heat treatment temperature results in an increase in particle size also.

The reason of the choice of 300% is as follows: samples containing 50% of DEGDA were prepared in order to crosslink a maximum of two mineral entities as shown earlier in Fig. 12. Samples containing 300% were investigated to ensure the full linking of the inorganic constituents (with every valency bond satisfied) on purpose, to explore the effect of this drastic crosslinker excess on the properties of the final materials. This results in a structure containing all possible links, which can be represented in the liquid phase as a hybrid polymer-like material, as described in Fig. 13.

In both cases, when using either 50% or 300% of DEGDA, the subsequent heat treatment causes the decomposition and oxidation of the organic part, and in this way the crosslinker acts as a catalyst of the inorganic condensation reaction. However, in the case when using 300% of DEGDA, the result is an even greater enlargement of both the particle size range and the sizes of the particles.

On the other hand, samples without crosslinker did not have any cross-linking agent at work among the mineral ions. Very homogeneous sols were obtained by hydrolysis, but this homogeneity

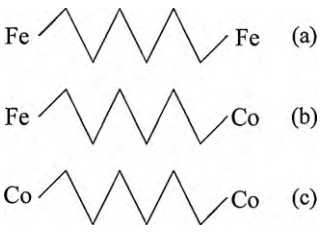

Fig. 12. The crosslinker probable reactions, (a) and (c) are unfavourable, and (b) is favourable.

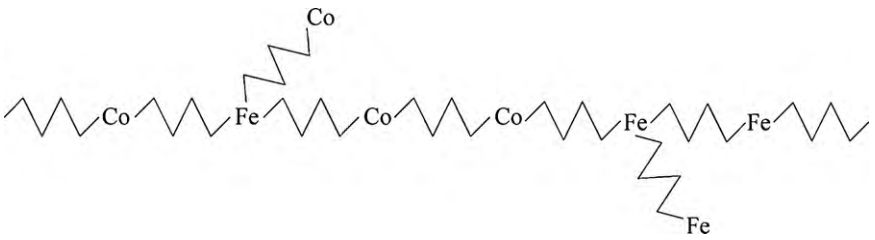

Fig. 13. The hybrid structure of materials containing 300% crosslinker.

did not last for long. At the gelling stage phase separation took place resulting also in a mixture of oxides, and because the mixing process was more random the result was a larger amount of the other oxides. The heat treatment was intended to form the ferrite lattice through an inter-diffusion process. However during this process, it was difficult for the cations to migrate between constituents to their thermodynamically ideal positions on A sites (tetrahedral) and B sites (octahedral) in the crystalline spinel lattice. The driving force for the inter-diffusion process was not sufficiently powerful due to the high degree of initial inhomogeneity in the amorphous powder, as demonstrated in the high levels of impurities in Fig. 2 samples 3 and 5.

4.2. Effect of the chelating agent

Chelating agents are usually used in inorganic chemistry to prevent particle agglomeration by reducing condensation reactions in liquid phase synthesis [26]. In our study, citric acid was used to chelate both inorganic precursors to form either monodendate or bidendate metal complexes [27], as shown in Fig. 14(a). In addition, it prevents both metal cations from undesired spontaneous condensation reactions.

From a structural point of view, it has been clearly observed that citric acid enables cobalt ferrite powders to be prepared under the same conditions as those when using the crosslinker. Indeed, comparisons of samples 2 with 10, and 4 with 12 show a decrease in the impurities' concentration from 3% to less than 1% respectively. Furthermore, the increase in the heat treatment temperature to 1000 °C, which was carried out when making sample 13, resulted in the single phase cobalt ferrite being obtained, without impurities, whereas the same high temperature did not produce the same level of purity even when 300% of DEGDA was used when making sample 9. In fact, increasing the CA concentration to 200% with respect to metal ions was sufficient to ensure the full chelation of the mineral ions forming both types of complex, and resulted in a more homogeneous mixture as shown in Fig. 14(b).

In addition, the inter-diffusion process during the heat treatment was enhanced due to the greater homogeneity, which had been achieved by that stage, and this enabled the development of pure cobalt ferrite material in sample 14, when applying a heat treatment temperature of only 600 °C. This can be explained by two facts: the first one is intimately associated with the molecular structure of the hybrid organic–inorganic complexes of both cobalt and iron ions, where, in contrast with the crosslinker, the chelating agent prevented any initial condensation or any cross-linking during the sol–gel synthesis. It causes the molecular structure of the sol to be composed of two hybrid complexes assigned by the initial stoichiometry as illustrated in Fig. 14(a). Although the complexes have been formed, the two species of complex are still free to diffuse throughout the sol. It is quite probable that the greater homogeneity is caused by an electrochemical effect, which would occur as follows. The strongly charged ferric ions would be partially neutralised by the citric acid anions, and would diffuse until they become surrounded evenly by the less strongly charged cobaltous ions also partially neutralised by the chelating agent. The process of diffusion would operate to ensure that the energy of the system would approach a minimum with no location having a higher or lower electrical charge. Therefore, because of the initial stoichiometry, one ion of cobalt would inevitably enter an environment where it is close to two ions of iron. This does not happen when using the crosslinker, because once one of the reactions (a), (b) or (c), illustrated in Fig. 12, has occurred, there is no mechanism for a rear-

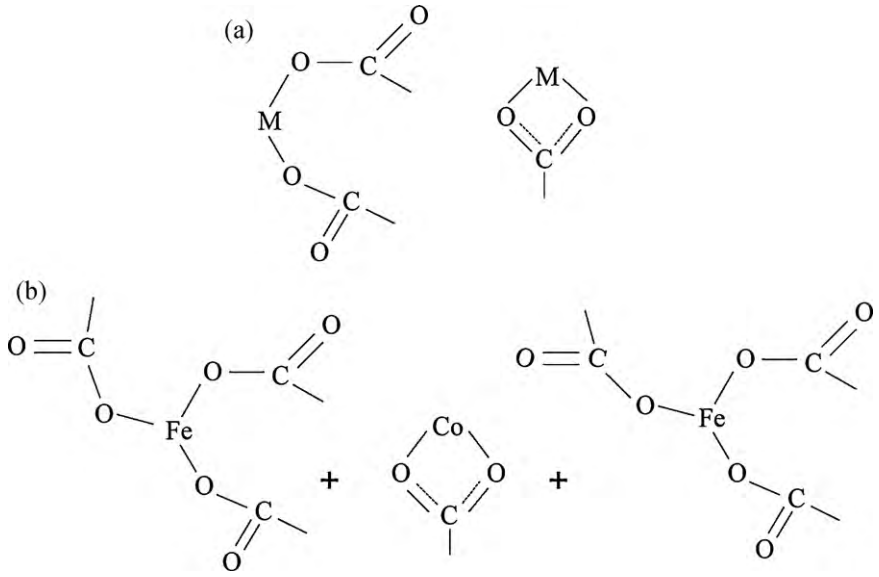

Fig. 14. (a) Metal complexes monodendate and bidendate and (b) organic–inorganic hybrids formed when using 200% chelating agent (CA).

rangement to take place to allow one ion of cobalt to be linked with two ions of iron. The second fact is that oxidation of the organic part of the hybrid complex during the heat treatment caused a further chemical reaction at this molecular unit level with the formation of cobalt ferrite structure, from a previously existing environment where the cobalt and iron ions were close to each other in the correct ratio. The critical difference between this and the crosslinker seems clearly to reside in the greater homogeneity at the molecular level which was not achieved to the same extent when using the crosslinker.

In all cases during the heat treatment, nanoparticles tended to agglomerate and form larger particles and this resulted in polydisperse powders as illustrated, for instance in Fig. 11. This particular example also seems to indicate that using larger quantities of the chelating agent while maintaining the same heat treatment temperature tends to produce larger particles, because some of the particles are larger than they are in the powder illustrated in Fig. 10 in which smaller amount of citric acid was used. The larger quantities of the chelating agent are required because smaller quantities of impurities are formed, but it seems that when larger quantities are used it may be important to lower the heat treatment temperature because even at 600 °C, there seems to be agglomeration forming larger particles. There is still a small window of opportunity because the DTA/TGA data indicates that the citric acid decomposes at about 190 °C. This suggests that a decrease in the temperature and the time of heat treatment would result in smaller particles, and a smaller size range, but there would still be the potential to achieve very low levels of impurities.

4.3. Calculating the crystal size of sample (14)

The crystal size of sample (14) was estimated using the Scherrer equation [28] as follows:

$$D = \frac{0.9 \times \lambda}{\delta \times \cos(2\theta)}$$

Substituting with respective values gives average crystal size of 45 [nm].

An estimate of the sizes of these particles using FE-SEM image in Fig. 11 gave values in the range from 20 nm to 250 nm. This indicates some particles in sample 14 are composed of a number of crystals i.e. polycrystalline, and some particles consist of individual crystals. The reason behind this is attributed to the high heat treatment temperature and the long dwelling time which facilitated the process of forming the larger particles at the expense of the smaller ones.

The analysis of the XRD pattern of sample 14 by (EVA) software provided with the instrument shows that the powder is composed of a single spinel phase of cobalt ferrite with lattice parameter (a) equal to 8.3919 Å.

5. Conclusions

Cobalt ferrite powders have been synthesized employing the sol–gel process. A particular focus was given to the investigation of the fundamental role of the crosslinker and chelating agent on the final structure and morphology of the materials obtained. It is clearly shown that citric acid enables the cobalt ferrite to be obtained with a higher purity than can be obtained using crosslinker. This difference has been correlated with the different molecular unit structures formed when using each of the two organic molecules. The crosslinker allows the formation of three different structural units which are a mixture of oxides (cobalt iron oxide, iron oxide, and cobalt oxide). On the other hand, the chelating agent permits the formation of individual molecular units that are free to diffuse, so that the initial stoichiometry can be maintained. In addition, the crosslinker and chelating agent were found to have a crucial effect on particle size and the extent of the range of different sizes of particles, under the same conditions. The results given in this paper can be considered as part of a preliminary study for the development of methods to prepare cobalt ferrite nanoparticles, and it is intended that they can be implemented in specific magnetic applications. Further study will be carried out on the development of methods to manufacture cobalt ferrite powder and the results will be presented in the future.

Acknowledgement

The financial support of University of Aleppo-(Syria) is gratefully acknowledged.

References

[1] C. Hou, H. Yu, Q. Zhang, Y. Li, H. Wang, J. Alloys Compd. 491 (2010) 431–435.
[2] R.C. Kambale, P.A. Shaikh, N.S. Harale, V.A. Bilur, Y.D. Kolekar, C.H. Bhosale, K.Y. Rajpure, J. Alloys Compd. 490 (2010) 568–571.
[3] L. Ai, J. Jiang, Curr. Appl. Phys. 10 (2010) 284–288.
[4] B.E. Kashevsky, V.E. Agabekov, S.B. Kashevsky, K.A. Kekalo, E.Y. Manina, I.V. Prokhorov, V.S. Ulashchik, Particuology 6 (2008) 322–333.
[5] R.M. Bozorth, E.F. Tilden, A.J. Williams, Phys. Rev. 99 (1955) 1788–1798.
[6] P.A. Shaikh, R.C. Kambale, A.V. Rao, Y.D. Kolekar, J. Alloys Compd. 492 (2010) 590–596.
[7] N.B. Ekreem, A.G. Olabi, T. Prescott, A. Rafferty, M.S.J. Hashmi, J. Mater. Process. Technol. 191 (2007) 96–101.
[8] A.G. Olabi, A. Grunwald, Mater. Des. 29 (2008) 469–483.
[9] A. Grunwald, A.G. Olabi, Sens. Actuators A: Phys. 144 (2008) 161–175.
[10] D.S. Mathew, R.-S. Juang, Chem. Eng. J. 129 (2007) 51–65.
[11] D.-H. Kim, D.E. Nikles, D.T. Johnson, C.S. Brazel, J. Magn. Magn. Mater. 320 (2008) 2390–2396.
[12] P.C. Morais, J. Alloys Compd. 483 (2009) 544–548.
[13] G. Baldi, D. Bonacchi, C. Innocenti, G. Lorenzi, C. Sangregorio, J. Magn. Magn. Mater. 311 (2007) 10–16.
[14] M. Gharagozlou, J. Alloys Compd. 486 (2009) 660–665.
[15] K. Maaz, A. Mumtaz, S.K. Hasanaina, A. Ceylan, J. Magn. Magn. Mater. 308 (2007) 289–295.
[16] V. Pillai, D.O. Shah, J. Magn. Magn. Mater. 163 (1996) 243–248.
[17] Z. Zi, Y. Sun, X. Zhu, Z. Yang, J. Dai, W. Song, J. Magn. Magn. Mater. 321 (2009) 1251–1255.
[18] Y. Chen, M. Ruan, Y.F. Jiang, S.G. Cheng, W. Li, J. Alloys Compd. 493 (2010) L36–L38.
[19] S. O'Brien, L. Brus, C.B. Murray, J. Am. Chem. Soc. 123 (2001) 12085–12086.
[20] E.V. Gopalan, P.A. Joy, I.A. Al-Omari, D.S. Kumar, Y. Yoshida, M.R. Anantharaman, J. Alloys Compd. 485 (2009) 711–717.
[21] S. Zhang, D. Dong, Y. Sui, Z. Liu, H. Wang, Z. Qian, W. Su, J. Alloy. Compd. 415 (2006) 257–260.
[22] R. Sen, G.C. Das, S. Mukherjee, J. Alloy. Compd. 490 (2010) 515–523.
[23] J.B. Silva, C.F. Diniz, J.D. Ardinson, A.I.C. Persiano, N.D.S. Mohallem, J. Magn. Magn. Mater. 272–276 (2004) e1851–e1853.
[24] C.J. Brinker, G.W. Scherer, Sol–Gel Science: The Physics and Chemistry of Sol–gel Processing, Academic Press, San Diego, 1990.
[25] A. Rafferty, T. Prescott, D. Brabazon, Ceram. Int. 34 (2008) 15–21.
[26] M. Oubaha, P. Etienne, S. Calas, P. Coudray, J.M. Nedelec, Y. Moreau, J. Sol–Gel Sci. Technol. 33 (2005) 241–248.
[27] P.C.R. Varma, J. Colreavy, J. Cassidy, M. Oubaha, B. Duffy, Prog. Org. Coat. 66 (2009) 406–411.
[28] M. George, S.S. Nair, A.M. John, P.A. Joy, M.R. Anantharaman, J. Phys. D: Appl. Phys. 39 (2006) 900–910.